ALUMINUM-FOR-IRON SUBSTITUTION, HYDROGEN BONDING, AND A NOVEL STRUCTURE-TYPE IN COQUIMBITE-LIKE MINERALS

Francesco DEMARTIN[§], Carlo CASTELLANO,
Carlo Maria GRAMACCIOLI AND Italo CAMPOSTRINI

*Dipartimento di Chimica Strutturale e Stereochimica Inorganica,
Università degli Studi di Milano, via Venezian 21, I–20133 Milano, Italy*

ABSTRACT

A single-crystal XRD study of coquimbite specimens from Vulcano Island, Italy, and from non-volcanic occurrences has confirmed the existence of a marked difference in the occupancy of the metal sites by Fe and Al. For compositions with a 1:1 Al:Fe ratio, a novel structure-type corresponding to the new mineral *aluminocoquimbite* was found, which demonstrates the different behavior of the Al and Fe in forming such complexes with H_2O and sulfate ions, respectively. The hydrogen-bond geometry was determined, and a peculiar cyclohexane-like arrangement of the H_2O molecules that do not coordinate the metal atoms has also been observed.

Keywords: coquimbite, aluminocoquimbite, new structure-type, single-crystal structure refinement, hydrogen bonds, Vulcano Island, Italy.

SOMMAIRE

Une étude par diffraction X de monocristaux de coquimbite provenant de l'île de Vulcano, en Italie, et d'indices non volcaniques a confirmé l'existence de différences dans le taux d'occupation des sites des métaux par Fe et Al. Pour les compositions ayant un rapport Al:Fe égal à 1:1, nous avons découvert un nouveau type de structure, adopté par la nouvelle espèce *aluminocoquimbite*, qui démontre le comportement distinct de Al et Fe dans la formation de tels complexes avec H_2O et les groupes sulfate, respectivement. Nous avons établi la géométrie des liaisons hydrogène, et nous mettons en évidence un agencement particulier de molécules de H_2O non liées aux atomes métalliques qui ressemble à l'agencement du cyclohexane.

(Traduit par la Rédaction)

Mots-clés: coquimbite, aluminocoquimbite, nouveau type de structure, structure affinée avec monocristal, liaisons hydrogène, île de Vulcano, Italie.

INTRODUCTION

Coquimbite, ideally $Fe^{3+}_2(SO_4)_3 \bullet 9H_2O$, is a secondary mineral found in the oxidized portions of iron sulfide deposits in arid regions, or associated with fumarolic activity. Because most samples reported in the literature show substitution of Al for Fe, its chemical formula is often written as $Fe_{2-x}Al_x(SO_4)_3 \bullet 9H_2O$.

The crystal structure of this trigonal mineral, space group $P\bar{3}1c$, was first solved by Fang & Robinson (1970) on a sample from Tierra Amarilla, Chile; it shows aluminum almost completely replacing iron at the 2*b* site (Al 0.90, Fe 0.10), whereas the 2*c* and 4*f* sites are exclusively occupied by iron. The same authors

clarified the polytypic relationship with paracoquimbite, which has a *c* parameter that is three times as large and space group $R\bar{3}$ (Robinson & Fang 1971, Fang & Robinson 1974).

A recent Rietveld refinement of the coquimbite structure, carried out by synchrotron powder X-ray diffraction, was performed by Majzlan *et al.* (2006) on a sample from the Richmond mine, Redding, California. It displays a similar type of substitution at the 2*b* site [Al 0.914(8), Fe 0.086(8)], together with minor replacement of iron by aluminum at the 4*f* site [Fe 0.928(8), Al 0.072(8)].

Renewed mineralogical interest in the fumarolic systems at Vulcano, Aeolian Islands, Sicily, Italy, has led

§ *E-mail address*: francesco.demartin@unimi.it

to the discovery of a number of rare and new minerals (*e.g.,* Garavelli *et al.* 2005, Campostrini *et al.* 2008, Demartin *et al.* 2009, Mitolo *et al.* 2009, Demartin *et al.* 2010, and references therein). During our systematic investigation on minerals from this island, we found excellent samples of coquimbite near the sea shore at the so-called "Grotta dell'Allume" (Alum Grotto), associated with voltaite, pertlikite, krausite, yavapaiite, pickeringite, tamarugite and metavoltine. Preliminary investigation of these samples of coquimbite, carried out by EDS microanalysis, showed variability in the Al:Fe ratio. In order to provide additional data about the distribution of Al and Fe in the structure, we decided to carry out crystal-structure refinements of selected specimens from different occurrences. As a result, we happened to find an Al-rich sample from Vulcano having a novel structure-type, therefore corresponding to a new mineral species. The latter was approved by the IMA Commission on New Minerals, Nomenclature and Classification [IMA #2009–095], as alumino-coquimbite. The description of the new species will be reported in a separate paper.

CHEMICAL AND X-RAY DATA

Together with two samples from Vulcano Island, Italy, designated as samples Vulc1 and Vulc2, respectively (the latter corresponding to the new mineral aluminocoquimbite), we investigated two additional specimens that formed in non-volcanic environments, *i.e.*, at La Alcaparrosa, Chile (sample Chile) and at the Dexter No. 7 mine, Calf Mesa, San Rafael Swell, Utah (sample Utah).

A preliminary chemical analysis was carried out on each of the same crystals used for structure deter-

mination and refinement with a JEOL JSM–5500 LV scanning electron microscope equipped with an IXRF EDS 2000 system (20 kV, 0.01 nA, 2 μm beam diameter). Element concentrations were measured using the $K\alpha$ lines for Al, Fe and S. The Al:Fe ratios (atomic) obtained are in agreement with the compositions independently derived from the structure refinement: they are, respectively, 1:3 for Vulc1 and Utah, 1:4.26 for Chile and 1:1 for Vulc2.

Selected crystallographic information, together with details concerning the data collection and refinement, are reported in Table 1. Intensity data corresponding to a complete scan of the Ewald sphere were collected using a Bruker Apex II diffractometer equipped with a 2K CCD detector and Mo$K\alpha$ radiation ($\lambda = 0.71073$ Å). The intensity data were reduced using the program SAINT (Bruker 2001), and corrected for Lorentz, polarization, and background effects. An absorption correction was applied using the SADABS program (Sheldrick 2000). All of the samples show the same space-group symmetry ($P\bar{3}1c$). The unit-cell parameters also are similar, and are consistent with those previously reported for coquimbite. The only exception is the Al-rich sample, Vulc2, for which the *a* parameter is about 0.2 Å shorter and the *c* parameter 0.2 Å longer than that of the other samples (Table 1).

The structures of Vulc1, Utah and Chile were refined, starting from the atomic positions reported by Fang & Robinson (1970), using the SHELXL97 program (Sheldrick 2008) implemented in the WINGX suite (Farrugia 1999). Scattering factors of the neutral atoms were used. Surprisingly, the same atomic coordinates did not give a satisfactory result for Vulc2 ($R = 0.477$) whose structure was instead solved by direct methods

TABLE 1. SINGLE-CRYSTAL DATA AND REFINEMENT DETAILS

$Fe_{2-x}Al_x(SO_4)_3 \cdot 9H_2O$	CHILE $x = 0.38$	UTAH $x = 0.50$	VULC1 $x = 0.50$	VULC2 $x = 1.00$
a (Å)	10.9370(4)	10.9170(5)	10.9100(7)	10.7065(7)
c (Å)	17.0813(7)	17.0829(8)	17.0625(11)	17.3077(11)
V (Å³)	1769.5(1)	1763.2(1)	1758.8(2)	1718.2(2)
μ (Mo$K\alpha$) (mm⁻¹)	1.815	1.733	1.737	1.399
D$_{calc}$ (g/cm³)	2.068	2.063	2.068	2.061
Range of data collection (°)	1.94<2θ<62.96	1.94<2θ<58.70	1.94<2θ<63.52	1.95<2θ<63.34
Scan mode	ω	ω	ω	ω
Measured reflections	17829	14126	18097	17595
Independent reflections	1917	1572	1939	1895
Observed reflections [*I* > 2σ(*I*)]	1717	1329	1567	1685
Parameters refined	109	108	108	108
Weighting parameters *a, b*	0.0439, 0.6146	0.0497, 0.2676	0.0532, 0.5490	0.0376, 0.7050
Final *R* and w*R*2	0.0220, 0.0734	0.0258, 0.0801	0.0351, 0.0882	0.0218, 0.0685
S	1.081	1.061	1.059	1.115

Notes: Trigonal, space group $P\bar{3}1c$, *Z* = 4.
$R = \Sigma||Fo| - |Fc|| / \Sigma|Fo|$; w$R2 = \{\Sigma[w(Fo^2 - Fc^2)^2] / \Sigma[w(Fo^2)^2]\}^{1/2}$; w = 1/[σ²($Fo^2$) + ($aq$)² + bq], where q = [max(0, Fo^2) + $2Fc^2$] / 3.
$S = \{\Sigma[w(Fo^2 - Fc^2)] / (n - p)\}^{1/2}$, where n is the number of reflections and p is the number of refined parameters.

using the Sir97 program (Altomare *et al.* 1999), and proved to be different from that of the other samples.

The occupancies of the three cation sites $M(1)$, $M(2)$ and $M(3)$ were also refined; for clarity in Tables 2–5, and in the Figures, the symbols $M(1)$, $M(2)$ and $M(3)$ are replaced by the corresponding symbol of the element prevailing in the site. The hydrogen atoms of the H_2O molecules were located in difference-Fourier maps and were included in the final refinements, with isotropic displacement parameters, whereas anisotropic displacement parameters were refined for all the other atoms. In all of the structures, the interstitial H_2O molecule displays two alternative orientations in which one of the two hydrogen atoms always occupies the same position (H21), whereas the other one (H22) statistically occupies two separate positions (H22a and H22b), each with an occupancy of 0.5.

The final coordinates and displacement parameters of the atoms are reported in Tables 2–5; interatomic distances are shown in Tables 6 and 7. Tables of observed and calculated structure-factors may be obtained from The Depository of Unpublished Data, on the MAC website [document Coquimbite-like minerals CM48_323].

RESULTS AND DISCUSSION

The structure of samples Vulc1, Utah and Chile is that already known for coquimbite (Fig. 1). An important feature is the non-equivalence of the three octahedrally coordinated metal sites. One of these, $M(1)$, is at the center of an isolated $M(1)(H_2O)_6$ octahedron, whereas another one, $M(2)$, is coordinated exclusively by sulfate ions, and $M(3)$, by three oxygen atoms of the sulfate ions and by three oxygen atoms of the H_2O molecules. Clusters with compositions $M(2)M(3)_2(SO_4)_6(H_2O)_6$ are formed by two $M(3)$- and one $M(2)$-centered octahedra and six SO_4 tetrahedra, which share only corners (Fig. 1). There are also six H_2O molecules that are held in the structure solely by hydrogen bonding.

In the previously reported structures (Fang & Robinson 1970, Majzlan *et al.* 2006), aluminum is the dominant metal at the $M(1)$ position, whereas iron is

TABLE 2. COORDINATES AND DISPLACEMENT PARAMETERS [$U_{eq}/U_{i,j}$] OF ATOMS IN Chile

Atom	Wyckoff notation	Site occupancy	X/a	Y/b	Z/c	U_{eq}
Al,Fe(1)	2*b*	Al 0.761(1)	0	0	0	0.01350(7)
		Fe 0.239(1)				
Fe(2)	2*c*	Fe 1.00	1/3	2/3	1/4	0.01147(4)
Fe(3)	4*f*	Fe 1.00	2/3	1/3	0.002498(9)	0.01703(3)
S	12*i*		0.244809(13)	0.415175(13)	0.123067(8)	0.01412(3)
O(1)	12*i*		0.31847(5)	0.34563(4)	0.09110(3)	0.02376(12)
O(2)	12*i*		0.10858(5)	0.31136(5)	0.15507(3)	0.02223(12)
O(3)	12*i*		0.21976(4)	0.49418(4)	0.06020(3)	0.02146(11)
O(4)	12*i*		0.33579(4)	0.51624(4)	0.18451(3)	0.01732(10)
OW(1)	12*i*		0.16668(4)	0.07066(4)	0.06225(3)	0.02367(12)
OW(2)	12*i*		0.44922(5)	0.11635(5)	0.20994(3)	0.03175(15)
OW(3)	12*i*		0.57200(5)	0.16221(5)	0.07123(3)	0.02949(13)
H11	12*i*		0.1851(7)	0.0205(6)	0.0924(5)	0.085(5)
H12	12*i*		0.2264(11)	0.1545(6)	0.0760(6)	0.073(4)
H21	12*i*		0.3722(6)	0.0384(6)	0.2091(7)	0.040(3)
H22a	12*i*	0.50	0.5068(5)	0.1020(8)	0.2363(6)	0.044(6)
H22b	12*i*	0.50	0.4342(7)	0.1729(6)	0.2362(5)	0.034(5)
H31	12*i*		0.5930(5)	0.0987(4)	0.0751(7)	0.060(4)
H32	12*i*		0.5317(7)	0.1528(10)	0.1142(3)	0.041(3)

Atom	U_{11}	U_{22}	U_{33}	U_{23}	U_{13}	U_{12}
Al,Fe(1)	0.01171(9)	0.01171(9)	0.01707(15)	0	0	0.00586(4)
Fe(2)	0.01087(5)	0.01087(5)	0.01265(8)	0	0	0.00544(2)
Fe(3)	0.01800(4)	0.01800(4)	0.01508(6)	0	0	0.00900(2)
S	0.01402(4)	0.01139(4)	0.01586(6)	-0.00226(4)	-0.00059(4)	0.00554(3)
O(1)	0.02056(15)	0.01930(15)	0.0325(2)	-0.00920(16)	-0.00008(17)	0.01076(11)
O(2)	0.01748(16)	0.01813(16)	0.0239(2)	0.00037(16)	-0.00309(16)	0.00352(12)
O(3)	0.02232(16)	0.01950(16)	0.01972(19)	0.00171(15)	-0.00414(15)	0.00832(12)
O(4)	0.01841(14)	0.01524(14)	0.01858(19)	-0.00573(13)	-0.00413(14)	0.00861(10)
OW(1)	0.02285(16)	0.01619(15)	0.0306(2)	-0.00207(15)	-0.00893(16)	0.00870(12)
OW(2)	0.0313(2)	0.0268(2)	0.0314(2)	-0.00226(19)	0.00318(19)	0.01032(16)
OW(3)	0.03932(19)	0.02753(17)	0.0273(2)	0.01067(16)	0.01408(18)	0.02098(13)

The exponent of the anisotropic displacement factor takes the form: $-2\pi^2[U_{11}h^2(a^*)^2 + ... + 2U_{12}hka^*b^* + ...]$; $U_{eq} = 1/3(U_{11} + U_{22} + U_{33})$.

TABLE 3. COORDINATES AND DISPLACEMENT PARAMETERS [U_{eq}/U_{ij}] OF ATOMS IN UTAH

Atom	Wyckoff notation	Site occupancy	X/a	Y/b	Z/c	U_{eq}
Al(1)	2b	Al 1.00	0	0	0	0.01316(13)
Fe(2)	2c	Fe 1.00	1/3	2/3	1/4	0.01144(6)
Fe(3)	4f	Fe 1.00	2/3	1/3	0.002517(12)	0.01706(5)
S	12i		0.244517(18)	0.414763(18)	0.122984(11)	0.01394(5)
O(1)	12i		0.31821(6)	0.34525(6)	0.09071(4)	0.02331(17)
O(2)	12i		0.10820(6)	0.31058(6)	0.15487(4)	0.02144(16)
O(3)	12i		0.21931(6)	0.49404(6)	0.06011(3)	0.02054(16)
O(4)	12i		0.33546(5)	0.51568(5)	0.18451(3)	0.01702(15)
OW(1)	12i		0.16438(5)	0.06998(6)	0.06151(4)	0.02145(16)
OW(2)	12i		0.44923(7)	0.11635(7)	0.20975(4)	0.0308(2)
OW(3)	12i		0.57172(6)	0.16237(6)	0.07102(4)	0.02932(18)
H11	12i		0.1831(6)	0.0150(5)	0.0869(5)	0.063(4)
H12	12i		0.2194(11)	0.1551(5)	0.0745(6)	0.050(4)
H21	12i		0.3735(7)	0.0379(6)	0.2063(7)	0.040(3)
H22a	12i	0.50	0.5162(9)	0.1104(9)	0.2314(7)	0.056(9)
H22b	12i	0.50	0.4202(6)	0.1623(6)	0.2356(6)	0.075(11)
H31	12i		0.5968(5)	0.1011(5)	0.0728(7)	0.055(4)
H32	12i		0.5318(8)	0.1471(13)	0.1152(3)	0.063(4)

Atom	U_{11}	U_{22}	U_{33}	U_{23}	U_{13}	U_{12}
Al(1)	0.01100(15)	0.01100(15)	0.0175(3)	0	0	0.00550(8)
Fe(2)	0.01042(7)	0.01042(7)	0.01348(12)	0	0	0.00521(4)
Fe(3)	0.01755(6)	0.01755(6)	0.01608(9)	0	0	0.00877(3)
S	0.01348(7)	0.01082(6)	0.01620(9)	-0.00228(6)	-0.00077(6)	0.00508(5)
O(1)	0.0195(2)	0.0187(2)	0.0328(3)	-0.0094(2)	-0.0003(2)	0.01033(16)
O(2)	0.0170(2)	0.0170(2)	0.0235(3)	-0.0002(2)	0.0030(2)	0.00338(18)
O(3)	0.0219(2)	0.0182(2)	0.0189(3)	0.0013(2)	-0.0036(2)	0.00809(17)
O(4)	0.0182(2)	0.0150(2)	0.0181(3)	-0.00564(19)	-0.0042(2)	0.00852(15)
OW(1)	0.0201(2)	0.0150(2)	0.0278(3)	-0.0017(2)	-0.0087(2)	0.00764(16)
OW(2)	0.0290(3)	0.0259(3)	0.0317(3)	-0.0030(3)	0.0029(3)	0.0094(2)
OW(3)	0.0388(3)	0.0275(2)	0.0275(3)	0.0098(2)	0.0137(3)	0.02090(19)

The exponent of the anisotropic displacement factor takes the form: $-2\pi^2[U_{11}h^2(a^*)^2 + ... + 2U_{12}hka^*b^*+...]$; $U_{eq} = 1/3(U_{11} + U_{22} + U_{33})$.
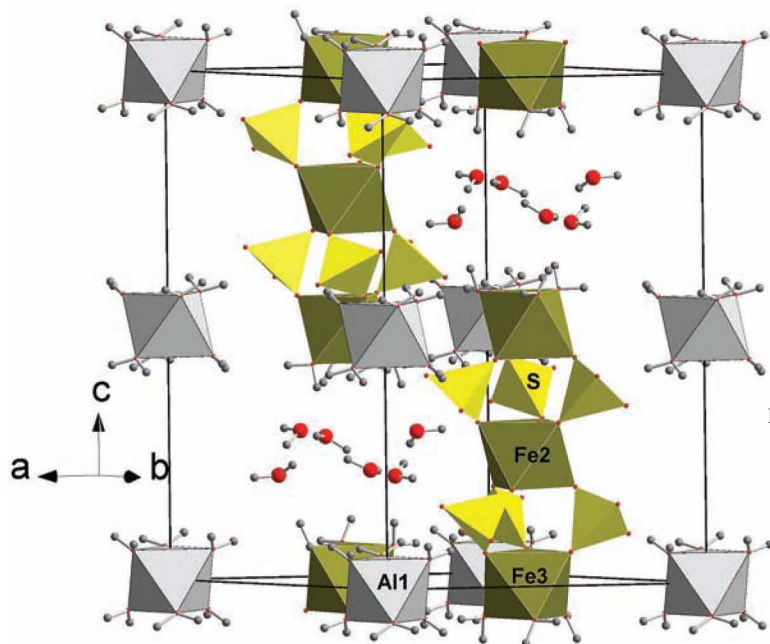
FIG. 1. A perspective view of the structure of coquimbite.

dominant in the other two sites. For Vulc1 and Utah, the refinement of the occupancies shows that the $M(1)$ site is occupied exclusively by aluminum, and the $M(2)$ and $M(3)$ sites are occupied only by iron. Therefore, in the final cycles of the refinement, these occupancies were kept fixed. For sample Chile, which displays a higher iron content, partial replacement of Al by Fe at the $M(1)$ site [Wyckoff position $2b$] is instead observed; the refined occupancies are 0.761(1) Al and 0.239(1) Fe.

Each $Fe_3(SO_4)_6(H_2O)_6$ cluster interacts through hydrogen bonds with its neighboring clusters, forming a discontinuous zig-zag chain along [001]. These chains, in turn, interact *via* hydrogen bonds with the isolated $Al(1)(H_2O)_6$ octahedra. This arrangement gives rise to cages containing the interstitial H_2O molecules [OW(2)] (Fig. 1). The hydrogen-bond pattern involving the H_2O molecules is shown in detail in Figure 2; it corresponds to that observed in the coquimbite-type compound $Fe_2(SeO_4)_3 \cdot 9H_2O$ (Giester & Miletich 1995). Of particular interest is the conformation of the group of the interstitial H_2O molecules, which resembles a cyclohexane-like chair (Fig. 3), with O⋯H distances within the chair in the range 1.90–1.96 Å (Table 6). Additional hydrogen-bond interactions with the remaining framework are observed between one equatorial atom of hydrogen of the chair (lone-pair acceptor) and one oxygen of a sulfate ion (lone-pair donor) and

between one hydrogen atom of the OW(3) molecule (lone-pair acceptor) and the OW(2) oxygen (lone-pair donor). The interatomic distances for these samples are given in Table 6. The mean S–O distance in the sulfate tetrahedron is statistically identical in all three samples (1.473 Å) and coincides with that found in gypsum (Pedersen & Semmingsen 1982), and in other minerals such as thermessaite (Demartin *et al*. 2008), where a similar corner-sharing arrangement of the sulfate ions is observed. The two S–O distances involving the oxygen atoms that are hydrogen-bonded to the Al-coordinated H_2O molecule OW(1) are the shortest, whereas the remaining two, which involve the oxygen atoms that coordinate iron, are significantly longer. This difference has also been observed in other sulfates (Graeber *et al*. 1965, Süsse 1968, Fanfani *et al*. 1970), and has been ascribed to an increase in S–O π-bonding as a result of a decrease in the negative charge on the oxygen atoms involved in hydrogen bonding.

The six Al(1)–OW(1) distances observed in samples Vulc1 and Utah are identical within the accuracy of structure refinements and in excellent agreement with the average Al–O distances, 1.881 Å, found in Vulc2, and 1.883 Å, found in other sulfates such as tamarugite (Robinson & Fang 1969); the same distances in sample Chile are slightly longer [1.9084(5) Å] because of partial replacement of aluminum by iron at this site.
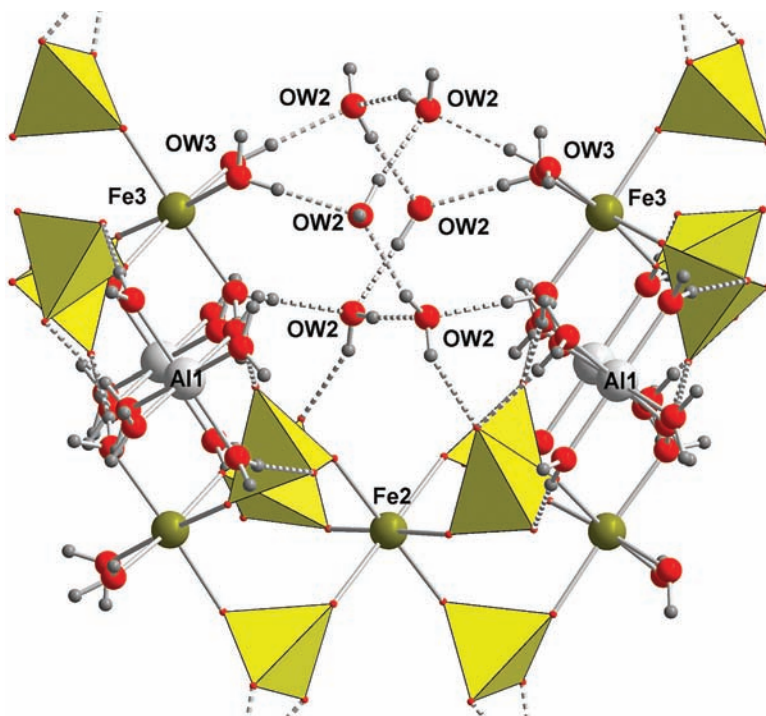
FIG. 2.   The hydrogen-bond pattern in coquimbite.

TABLE 4. COORDINATES AND DISPLACEMENT PARAMETERS [U_{eq}/U_{ij}] OF ATOMS IN Vulc1

Atom	Wyckoff notation	Site occupancy	X/a	Y/b	Z/c	U_{eq}
Al(1)	2b	Al 1.00	0	0	0	0.01276(13)
Fe(2)	2c	Fe 1.00	1/3	2/3	1/4	0.01068(6)
Fe(3)	4f	Fe 1.00	2/3	1/3	0.002502(13)	0.01723(5)
S	12i		0.244618(19)	0.414813(19)	0.122883(12)	0.01328(5)
O(1)	12i		0.31831(6)	0.34528(6)	0.09069(4)	0.02288(17)
O(2)	12i		0.10784(6)	0.31042(7)	0.15472(4)	0.02127(17)
O(3)	12i		0.21952(6)	0.49428(6)	0.06010(4)	0.02057(17)
O(4)	12i		0.33561(6)	0.51557(6)	0.18440(4)	0.01649(15)
OW(1)	12i		0.16433(6)	0.06986(6)	0.06158(4)	0.02104(16)
OW(2)	12i		0.44934(7)	0.11625(7)	0.20976(5)	0.0307(2)
OW(3)	12i		0.57197(7)	0.16249(7)	0.07096(4)	0.02909(19)
H11	12i		0.1828(7)	0.0143(5)	0.0866(5)	0.063(5)
H12	12i		0.2182(13)	0.1551(5)	0.0749(7)	0.058(5)
H21	12i		0.3721(7)	0.0379(7)	0.2081(8)	0.042(4)
H22a	12i	0.50	0.5170(5)	0.1125(9)	0.2319(7)	0.041(8)
H22b	12i	0.50	0.4203(6)	0.1621(6)	0.2362(6)	0.090(14)
H31	12i		0.5964(5)	0.1003(5)	0.0732(8)	0.052(4)
H32	12i		0.5298(9)	0.1448(16)	0.1145(3)	0.067(5)

Atom	U_{11}	U_{22}	U_{33}	U_{23}	U_{13}	U_{12}
Al(1)	0.01039(15)	0.01039(15)	0.0175(3)	0	0	0.00520(8)
Fe(2)	0.00999(7)	0.00999(7)	0.01206(11)	0	0	0.00500(3)
Fe(3)	0.01792(6)	0.01792(6)	0.01584(9)	0	0	0.00896(3)
S	0.01313(6)	0.01027(6)	0.01524(8)	-0.00241(6)	-0.00073(6)	0.00495(5)
O(1)	0.0198(2)	0.0181(2)	0.0321(3)	-0.0099(2)	-0.0001(2)	0.01051(17)
O(2)	0.0165(2)	0.0175(2)	0.0230(3)	-0.0003(2)	0.0032(2)	0.00328(18)
O(3)	0.0212(2)	0.0194(2)	0.0183(3)	0.0012(2)	-0.0044(2)	0.00812(18)
O(4)	0.0180(2)	0.0146(2)	0.0179(3)	-0.0055(2)	-0.0040(2)	0.00896(15)
OW(1)	0.0198(2)	0.0141(2)	0.0280(3)	-0.0016(2)	-0.0084(2)	0.00756(16)
OW(2)	0.0292(3)	0.0263(3)	0.0308(3)	-0.0022(3)	0.0034(3)	0.0095(2)
OW(3)	0.0386(3)	0.0275(2)	0.0276(3)	0.0100(2)	0.0136(3)	0.02129(19)

The exponent of the anisotropic displacement factor takes the form: $-2\pi^2[U_{11}h^2(a^*)^2 + \ldots + 2U_{12}hka^*b^* + \ldots]$;
$U_{eq} = 1/3(U_{11} + U_{22} + U_{33})$.
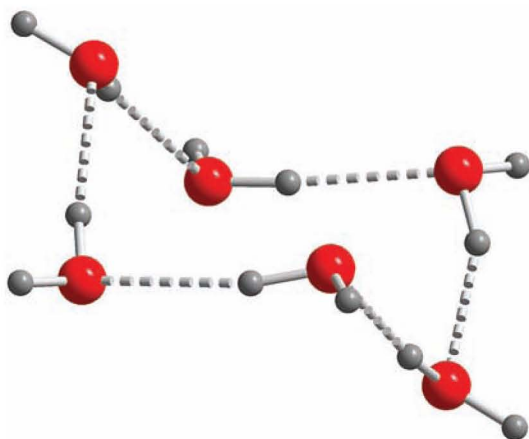
FIG. 3.   The cyclohexane-like chair arrangement of the cage-trapped H_2O molecules.

The Fe(2)–O distances are statistically identical in all three samples and are in excellent agreement with the average Fe–O distance found by Fang & Robinson (1970) for this site, which is occupied exclusively by iron. Similar results were found for the Fe(3)–O(3) and Fe(3)–OW(3) distances, which also are consistent with the exclusive presence of iron at this site. An important feature of these structures is that aluminum is invariably coordinated by H_2O, whereas iron is coordinated by sulfate ions and H_2O.

The structure of the Al-rich sample Vulc2 is different from that of the other samples (Figs. 4, 5). It contains octahedrally coordinated iron atoms, Fe(1) and Fe(2), exclusively linked to the oxygen atoms of the sulfate ions; in addition, an Al(3)(H_2O)$_6$ unit and interstitial H_2O molecules are present. The site-occupancy refinement shows that the Fe(1) and Fe(2) positions are occupied by iron, and the Al(3) site, by aluminum. The Fe(1) and Fe(2) octahedra are connected to sulfate tetrahedra by corner-sharing and alternate to form
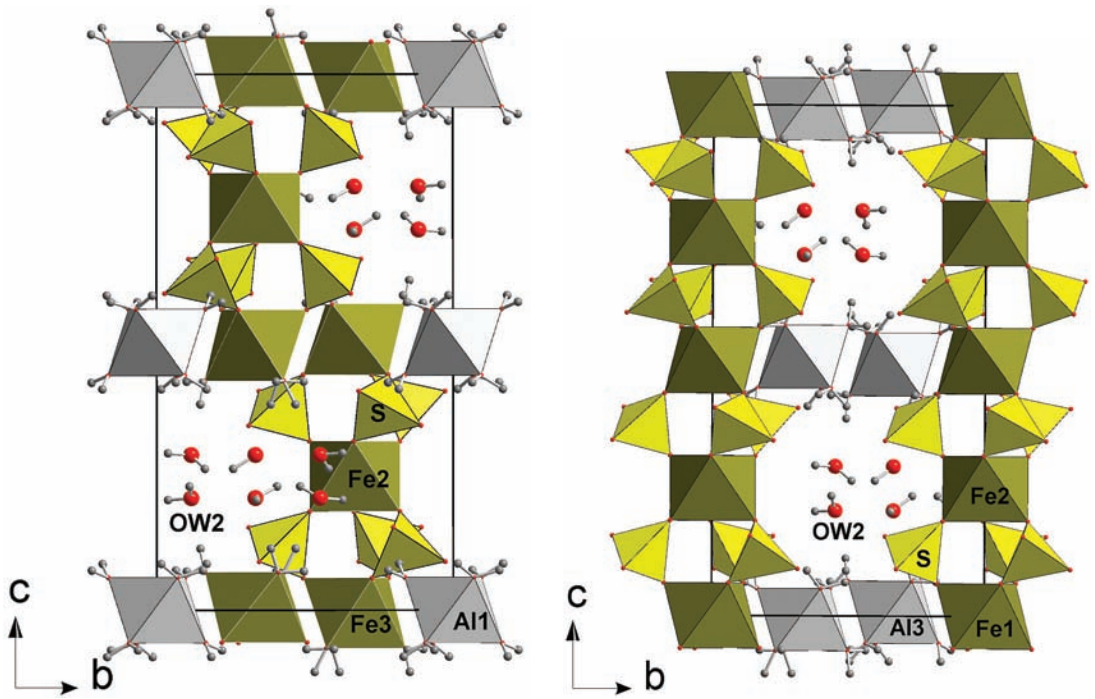
FIG. 4.   A comparative view of the coquimbite (left) and Vulc2 (right) structures projected along [100].
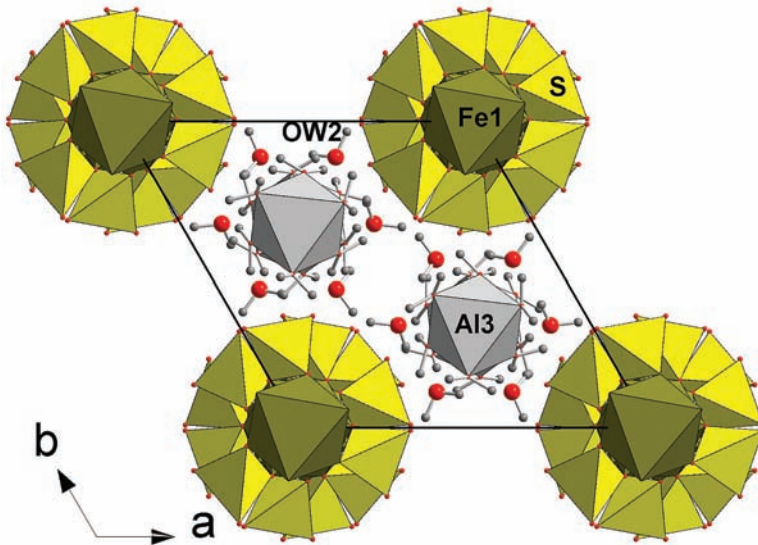
FIG. 5.   A view of the Vulc2 structure projected along [001].

TABLE 5. COORDINATES AND DISPLACEMENT PARAMETERS [U_{eq}/U_{ij}] OF ATOMS IN Vulc2

Atom	Wyckoff notation	Site occupancy	X/a	Y/b	Z/c	U_{eq}
Fe(1)	2b	Fe 1.00	0	0	0	0.01458(11)
Fe(2)	2a	Fe 1.00	0	0	1/4	0.01099(10)
Al(3)	4f	Al 1.00	2/3	1/3	-0.00824(4)	0.01503(14)
S	12i		0.25531(3)	0.16880(3)	0.124832(17)	0.01293(9)
O(1)	12i		0.17500(11)	0.06030(11)	0.06406(5)	0.0191(2)
O(2)	12i		0.36509(11)	0.14054(12)	0.15622(6)	0.0203(2)
O(3)	12i		0.32365(11)	0.31459(11)	0.09212(7)	0.0220(2)
O(4)	12i		0.15347(10)	0.15841(10)	0.18631(5)	0.01637(19)
OW(1)	12i		0.56588(11)	0.16639(11)	0.05370(6)	0.0214(2)
OW(2)	12i		0.45162(13)	0.33483(14)	0.79333(7)	0.0299(3)
OW(3)	12i		0.50030(12)	0.26571(12)	-0.06857(7)	0.0230(2)
H11	12i		0.508(2)	0.159(3)	0.0888(11)	0.049(7)
H12	12i		0.610(2)	0.121(2)	0.0659(14)	0.051(7)
H21	12i		0.378(2)	0.345(3)	0.7951(15)	0.055(8)
H22a	12i	0.50	0.511(4)	0.403(3)	0.765(2)	0.039(13)
H22b	12i	0.50	0.438(5)	0.266(4)	0.765(2)	0.043(14)
H31	12i		0.491(3)	0.295(3)	-0.1129(8)	0.051(7)
H32	12i		0.435(2)	0.1770(13)	-0.0672(16)	0.070(9)

Atom	U_{11}	U_{22}	U_{33}	U_{23}	U_{13}	U_{12}
Fe(1)	0.01610(15)	0.01610(15)	0.0115(2)	0	0	0.00805(7)
Fe(2)	0.01102(13)	0.01102(13)	0.01092(19)	0	0	0.00551(7)
Al(3)	0.0127(2)	0.0127(2)	0.0196(3)	0	0	0.00636(10)
S	0.01124(14)	0.01361(14)	0.01375(14)	0.00182(10)	0.00157(9)	0.00607(11)
O(1)	0.0186(5)	0.0233(5)	0.0161(4)	-0.0042(4)	-0.0024(4)	0.0110(4)
O(2)	0.0175(5)	0.0252(5)	0.0217(5)	0.0023(4)	-0.0015(4)	0.0132(4)
O(3)	0.0188(5)	0.0174(5)	0.0297(5)	0.0099(4)	0.0088(4)	0.0091(4)
O(4)	0.0153(4)	0.0158(5)	0.0161(4)	0.0010(3)	0.0050(3)	0.0062(4)
OW(1)	0.0192(5)	0.0197(5)	0.0279(5)	0.0075(4)	0.0062(4)	0.0118(4)
OW(2)	0.0246(6)	0.0331(6)	0.0326(6)	0.0042(5)	0.0019(5)	0.0147(5)
OW(3)	0.0190(5)	0.0182(5)	0.0276(6)	0.0010(4)	-0.0064(4)	0.0062(4)

The exponent of the anisotropic displacement factor takes the form: $-2\pi^2[U_{11}h^2(a^*)^2 + ... + 2U_{12}hka^*b^* + ...]$; $U_{eq} = 1/3(U_{11} + U_{22} + U_{33})$.
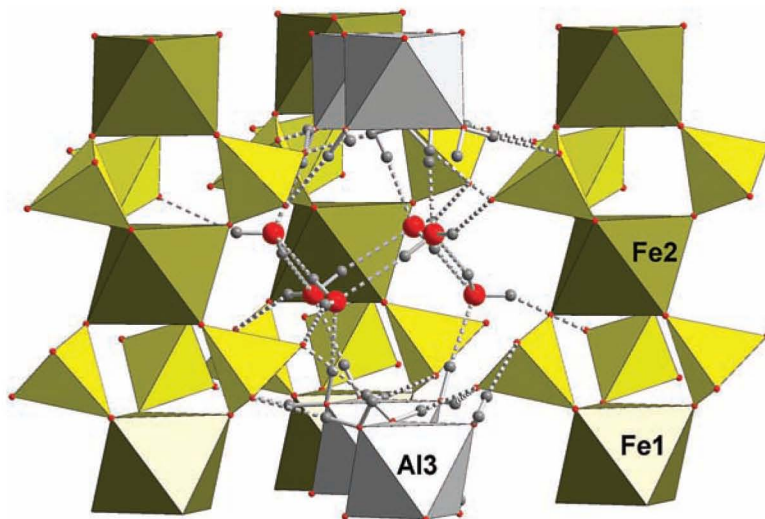
FIG. 6. A view of the hydrogen-bond pattern in Vulc2.

infinite columns along [001], similar to those observed in ferrinatrite, $Na_3(H_2O)_3[Fe(SO_4)_3]$ (Scordari 1977, Scordari & Venturi 2009]. These columns are joined through hydrogen-bond interactions with the octahedral $Al(3)(H_2O)_6$ units, which are located at about $z = 0, 1/2$, 1, *etc*. As a result, the structure displays cages centered at about $z = ¼$ and $¾$, which are occupied by six H_2O molecules [OW(2) and its symmetry equivalents] joined by hydrogen bonds and arranged in a cyclohexane-like chair conformation similar to that observed in the structure of coquimbite (Fig. 6). Additional hydrogen bonds involving these H_2O molecules are formed with the surrounding sulfate ions, whose oxygen atoms are lone-pair donors, and with the Al(3) coordinated H_2O molecules, whose hydrogen atoms are lone-pair acceptors (Table 7).

TABLE 6. INTERATOMIC DISTANCES (Å) AND ANGLES (°) FOR Al-POOR SAMPLES

	Chile	Utah	Vulc1
Al(1) – OW(1) × 6	1.9084(5)	1.8808(6)	1.8796(6)
Fe(2) – O(4) × 6	2.0008(5)	2.0018(6)	2.0029(7)
Fe(3) – O(3) × 3	1.9763(4)	1.9747(5)	1.9710(6)
Fe(3) – OW(3) × 3	2.0038(5)	1.9982(6)	1.9950(7)
S – O(1)	1.4623(6)	1.4621(7)	1.4607(8)
S – O(2)	1.4547(4)	1.4534(5)	1.4558(6)
S – O(3)	1.4871(5)	1.4888(7)	1.4870(7)
S – O(4)	1.4878(4)	1.4867(5)	1.4847(6)
S – O (average)	1.473	1.473	1.472
OW(1) – Al(1) – OW(1) × 6	88.03(2)	88.18(3)	88.21(3)
OW(1) – Al(1) – OW(1) × 6	91.97(2)	91.82(3)	91.79(3)
OW(1) – Al(1) – OW(1) × 3	180.00(3)	180.00(4)	180.00(4)
O(4) – Fe(2) – O(4) × 3	87.26(3)	87.37(3)	87.31(4)
O(4) – Fe(2) – O(4) × 3	89.18(2)	89.03(3)	89.08(3)
O(4) – Fe(2) – O(4) × 6	91.784(18)	91.81(2)	91.81(3)
O(4) – Fe(2) – O(4) × 3	178.66(2)	178.85(3)	178.77(3)
O(3) – Fe(3) – O(3) × 3	84.78(2)	84.77(3)	84.74(3)
O(3) – Fe(3) – O(3) × 3	92.85(2)	92.83(3)	92.86(3)
O(3) – Fe(3) – O(3) × 3	93.408(18)	93.43(2)	93.41(3)
O(3) – Fe(3) – O(3) × 3	173.57(2)	173.58(3)	173.56(3)
OW(3) – Fe(3) – OW(3) × 3	89.15(2)	89.17(3)	89.08(3)
O(2) – S – O(1)	110.48(3)	110.43(4)	110.43(4)
O(2) – S – O(3)	108.09(3)	108.11(4)	108.02(4)
O(2) – S – O(4)	111.00(3)	110.98(3)	111.08(4)
O(1) – S – O(3)	110.00(3)	109.83(4)	109.97(4)
O(1) – S – O(4)	108.18(3)	108.32(4)	108.21(4)
O(4) – S – O(3)	109.08(3)	109.16(3)	109.12(4)
Hydrogen bonds			
OW(1)⋯O(1)	2.655(1)	2.656(1)	2.655(1)
OW(1) – H12⋯O(1)	163.3(5)	169.6(5)	170.3(5)
OW(1)⋯OW(2)	2.645(1)	2.643(1)	2.642(1)
OW(3) – H32⋯OW(2)	173.4(5)	179.2(6)	176.5(6)
OW(1)⋯O(2)ⁱ	2.699(1)	2.703(1)	2.696(1)
OW(1) – H11⋯O(2)ⁱ	172.6(7)	170.6(6)	170.2(6)
OW(2)⋯O(2)ⁱ	2.750(1)	2.747(1)	2.743(1)
OW(2) – H21⋯O(2)ⁱ	152.1(6)	155.5(6)	153.1(7)
OW(2)⋯OW(2)ⁱⁱ	2.735(1)	2.735(1)	2.735(1)
OW(2) – H22b⋯OW(2)ⁱⁱ	165.5(6)	152.5(7)	152.3(7)
OW(2)⋯OW(2)ⁱⁱⁱ	2.748(1)	2.748(1)	2.742(1)
OW(2) – H22a⋯OW(2)ⁱⁱⁱ	166.2(7)	171.7(8)	173.8(8)
OW(3)⋯O(1)ⁱᵛ	2.661(1)	2.662(1)	2.658(1)
OW(3) – H31⋯O(1)ᵛ	173.6(5)	172.2(5)	172.8(5)

Symmetry codes: i = –x + y, –x, z; ii = x, x – y, 1/2 – z; iii = 1 – x + y, y, 1/2 – z; iv = 1 – y, x – y, z.

A comparison between the structures of coquimbite and Vulc2 is shown in Figures 4a and 4b, respectively. The structure of Vulc2 can be derived from the other one by translating the $Fe(2)(SO_4)_6$ building blocks and the nearby H_2O molecules along the vector $[\bar{3}, \bar{2}, 0]$. In view of the preference of aluminum to coordinate H_2O molecules and of iron to coordinate sulfate ions, this translation implies a change in the contents of the various sites. In particular, the $M(1)$ site, which is completely surrounded by H_2O in coquimbite, is instead surrounded by sulfate groups in Vulc2, and the $M(3)$ site becomes entirely surrounded by H_2O groups. As the full occupancy of the $M(1)$ and $M(2)$ sites corresponds to 0.5 *apfu* each, and that of $M(3)$ to 1.0 *apfu*, the chemical composition of Vulc2 corresponds to a 1:1 overall atomic ratio of Al and Fe, instead of 1:3 or less as for the other cases. In other words, considering all the possibilities, the observed atomic ratio 1:1 can only be achieved in two ways: a) by filling completely the $M(1)$ and $M(2)$ sites with aluminum and $M(3)$ with iron, or b) by filling completely $M(1)$ and $M(2)$ with iron and $M(3)$ with aluminum. Taking into account the fact that iron prefers to be coordinated to the sulfate ions, whereas aluminum prefers coordination to H_2O molecules, the second case is more favorable because Fe(2) is completely surrounded by sulfate ions.

Conclusions

For coquimbite, the formula $Fe_{2-x}Al_x(SO_4)_3•9H_2O$ or the "traditional" one $Fe_2(SO_4)_3•9H_2O$ would suggest the possibility of a wide range of continuous replacement of Fe^{3+} by other ions of similar radius, such as especially aluminum, without modifying the structural type. However, the behavior of the metals at the various sites differs in important ways, so that replacement of iron with aluminum is more selective. This effect is so strong that on increasing the Al content beyond a certain limit, a structural rearrangement of the phase occurs, leading to the new mineral species *aluminocoquimbite*. Structural changes in response to the occupancy of the isolated or "free" octahedral sites, similar to those here described, have also been observed in the copiapite-group minerals (Majzlan & Michallik 2007), and are likely to occur in other open structures.

References

Altomare, A., Burla, M.C., Camalli, M., Cascarano, G., Giacovazzo, C., Gagliardi, A., Moliterni, A.G.,

TABLE 7. INTERATOMIC DISTANCES (Å) AND ANGLES (°) FOR Vᴜʟᴄ2

Fe(1) – O (1) × 6	1.9867(10)	O(1) – Fe(1) – O(1) × 6	88.12(4)
Fe(2) – O(4) × 6	2.0012(10)	O(1) – Fe(1) – O(1) × 6	91.88(4)
Al(3) – OW(1) × 3	1.8920(11)	O(1) – Fe(1) – O(1) × 3	180.00(8)
Al(3) – OW(3) × 3	1.8702(11)		
		O(4) – Fe(2) – O(4) × 3	85.56(5)
S – O(1)	1.4819(10)	O(4) – Fe(2) – O(4) × 3	89.35(6)
S – O(2)	1.4573(10)	O(4) – Fe(2) – O(4) × 6	92.57(4)
S – O(3)	1.4663(11)	O(4) – Fe(2) – O(4) × 3	177.38(5)
S – O(4)	1.4874(9)		
S – O (average)	1.473	OW(1) – Al(3) – OW(1) × 3	91.05(5)
		OW(1) – Al(3) – OW(3) × 3	88.15(5)
O(1) – S – O(2)	108.30(6)	OW(1) – Al(3) – OW(3) × 3	88.94(5)
O(1) – S – O(3)	110.21(7)	OW(3) – Al(3) – OW(3) × 3	91.86(6)
O(1) – S – O(4)	109.44(6)	OW(1) – Al(3) – OW(3) × 3	179.20(5)
O(2) – S – O(3)	109.87(6)		
O(2) – S – O(4)	110.79(6)		
O(3) – S – O(4)	108.22(6)		

Hydrogen bonds

OW(1)···O(2)	2.693(2)	OW(1) – H11···O(2)	173(2)
OW(1)···O(3)ⁱ	2.660(2)	OW(1) – H12···O(3)ⁱ	174(1)
OW(2)···O(2)ⁱⁱ	2.751(2)	OW(2) – H21···O(2)ⁱⁱ	157(2)
OW(2)···OW(2)ⁱⁱⁱ	2.734(2)	OW(2) – H22a···OW(2)ⁱⁱⁱ	172(4)
OW(2)···OW(2)ⁱᵛ	2.775(2)	OW(2) – H22b···OW(2)ⁱᵛ	166(4)
OW(3)···O(3)ᵛ	2.631(2)	OW(3) – H32···O(3)ᵛ	163(1)
OW(3)···OW(2)ᵛⁱ	2.630(2)	OW(3) – H31···OW(2)ᵛⁱ	173(2)

Symmetry codes: i = 1 – y, x – y, z; ii = x – y, x, 1 – z; iii = 1 – y, 1 – x, 3/2 – z; iv = x, x – y, 3/2 – z; v = y, y – x, –z; vi = x, y, z – 1.

Polidori, G. & Spagna, R. (1999): Sɪʀ97, a new tool for crystal structure determination and refinement. *J. Appl. Crystallogr.* **32**, 115-119.

Bruker (2001): Sᴍᴀʀᴛ and Sᴀɪɴᴛ. Bruker AXS Inc., Madison, Wisconsin, U.S.A.

Campostrini, I., Demartin, F., Gramaccioli, C.M. & Orlandi, P. (2008): Hephaistosite, TlPb₂Cl₅, a new thallium mineral species from La Fossa crater, Vulcano, Aeolian Islands, Italy. *Can. Mineral.* **46**, 701-708.

Demartin, F., Gramaccioli, C.M. & Campostrini, I. (2008): Thermessaite, K₂[AlF₃|SO₄], a new ino-aluminofluoride sulfate from La Fossa crater, Vulcano, Aeolian Islands, Italy. *Can. Mineral.* **46**, 693-700.

Demartin, F., Gramaccioli, C.M. & Campostrini, I. (2009): Steropesite, Tl₃BiCl₆, a new thallium bismuth chloride from La Fossa crater, Vulcano, Aeolian Islands, Italy. *Can. Mineral.* **47**, 373-380.

Demartin, F., Gramaccioli, C.M., Campostrini, I. & Pilati T. (2010): Aiolosite, Na₂(Na₂Bi)(SO₄)₃Cl, a new sulfate isotypic to apatite from La Fossa Crater, Vulcano, Aeolian Islands, Italy. *Am. Mineral.* **95**, 382-385.

Fanfani, L., Nunzi, A. & Zanazzi, P.F. (1970): The crystal structure of roemerite. *Am. Mineral.* **55**, 78-89.

Fang, J.H. & Robinson, P.D. (1970): Crystal structures and mineral chemistry of hydrated ferric sulfates. I. The crystal structure of coquimbite. *Am. Mineral.* **55**, 1534-1540.

Fang, J.H. & Robinson, P.D. (1974): Polytypism in coquimbite and paracoquimbite. *Neues Jahrb. Mineral., Monatsh.*, 89-91.

Farrugia, L. J. (1999): WɪɴɢX suite for small-molecule single-crystal crystallography. *J. Appl. Crystallogr.* **32**, 837-838.

Garavelli, A., Mozgova, N.N., Orlandi, P., Bonaccorsi, E., Pinto, D., Moëlo, Y. & Borodaev, Yᴜ.S. (2005): Rare sulfosalts from Vulcano, Aeolian Islands, Italy. VI. Vurroite Pb₂₀Sn₂(Bi,As)₂₂S₅₄Cl₆, a new mineral species. *Can. Mineral.* **43**, 703-711.

Giester, G. & Miletich, R. (1995): Crystal structure and thermal decomposition of the coquimbite-type compound Fe₂(SeO₄)₃•9H₂O. *Neues Jahrb. Mineral., Monatsh.*, 211-223.

Graeber, E.J., Morosin, B. & Rosenzweig, A. (1965): The crystal structure of krausite, KFe(SO₄)₂•H₂O. *Am. Mineral.* **50**, 1929-1936.

Majzlan, J. & Michallik, R. (2007): The crystal structures, solid solutions and infrared spectra of copiapite-group minerals. *Mineral. Mag.* **71**, 557-573.

Majzlan, J., Navrotsky, A., McCleskey, R.B. & Alpers, C.N. (2006): Thermodynamic properties and crystal structure refinement of ferricopiapite, coquimbite, rhomboclase, and Fe₂(SO₄)₃(H₂O)₅. *Eur. J. Mineral.* **18**, 175-186.

MITOLO, D., PINTO, D., GARAVELLI, A., BINDI, L. & VURRO, F. (2009): The role of the minor substitutions in the crystal structure of natural challacolloite, KPb_2Cl_5, and hephaistosite, $TlPb_2Cl_5$, from Vulcano (Aeolian Archipelago, Italy). *Mineral. Petrol.* **96**, 121-128.

PEDERSEN, B.F. & SEMMINGSEN, D. (1982): Neutron diffraction refinement of the structure of gypsum, $CaSO_4 \cdot 2H_2O$. *Acta Crystallogr.* **B38**, 1074-1077.

ROBINSON, P.D. & FANG, J.H. (1969): Crystal structures and mineral chemistry of double-salts hydrates. I. Direct determination of the crystal structure of tamarugite. *Am. Mineral.* **54**, 19-30.

ROBINSON, P.D. & FANG, J.H. (1971): Crystal structures and mineral chemistry of hydrated ferric sulphates. II. The crystal structure of paracoquimbite. *Am. Mineral.* **56**, 1567-1572.

SCORDARI, F. (1977): The crystal structure of ferrinatrite, $Na_3(H_2O)_3[Fe(SO_4)_3]$ and its relationship to Maus's salt, $(H_3O)_2K_2\{K_{0.5}(H_2O)_{0.5}\}_6[Fe_3O(H_2O)_3(SO_4)_6](OH)_2$. *Mineral. Mag.* **41**, 375-383.

SCORDARI, F. & VENTRUTI, G. (2009): Sideronatrite, $Na_2Fe(SO_4)_2(OH) \cdot 3H_2O$: crystal structure of the orthorhombic polytype and OD character analysis. *Am. Mineral.* **94**, 1679-1686.

SHELDRICK, G.M. (2000): SADABS *Area-Detector Absorption Correction Program*. Bruker AXS Inc., Madison, Wisconsin, U.S.A.

SHELDRICK, G.M. (2008): A short history of SHELX. *Acta Crystallogr.* **A64**, 112-122.

SÜSSE, P. (1968): The crystal structure of amarantite, $Fe_2(SO_4)_2O \cdot 7H_2O$. *Z. Kristallogr.* **127**, 261-275.